Feasibility study of the magnetic beam self-focusing phenomenon in a stack of conducting foils: application to TNSA proton beams

P.A. Ni, F.M. Bieniosek and B.G. Logan,
Lawrence Berkeley National Laboratory, Berkeley, CA, USA

R.H. Cohen and S.M. Lund,
Lawrence Livermore National Laboratory, Livermore, CA, USA

M. Roth and G. Schaumann.
TU-Darmstadt, Germany

N. Alexander
General Atomics, San Diego, CA, USA

Keywords: particle beam self-focusing, magnetic pinch, TNSA proton beam focusing, proton fast ignition, TNSA proton beam collimation.

Abstract
This paper investigates prospects of utilizing a high-power laser-driven target-normal-sheath-acceleration (TNSA) proton beam for the experimental demonstration of the magnetic self-focusing phenomenon in charged particle beams. In the proposed concept, focusing is achieved by propagating a space-charge dominated ion beam through a stack of thin conducting and grounded foils separated by vacuum gaps. As the beam travels through the system, image charges build up at the foils and generate electric field that counteracts the beam's electrostatic self-field – a dominant force responsible for expansion of a high current beam. Once the electrostatic self-field is "neutralized" by the image charges, the beam current's magnetic self-field will do the focusing. The focal spot size and focal length depends on the choice of a number of foils and distance between foils. Considering the typical electrical current level of a TNSA proton beam, we conclude that it is feasible to focus or collimate a beam within tens of millimeters distance, e.g., using 200-1000 Al foils, 0.5 μm thick each, with foil spacing ranging from 25 μm to 100 μm. These requirements are within technical capabilities of modern target fabrication, thus allowing the first possible demonstration of the pinch effect with heavy ion beams.

1. Introduction

Focusing and transport of space-charge-dominated, hundreds of kilo-Amperes, ion beams are challenging problems, because the strong repulsive Coulomb force between ions leads to rapid expansion of the beam envelope. This space charge phenomenon is an important issue in a large number of applications, including proton-based fast ignition, heavy-ion fusion drivers, isochoric heating of matter in high energy density laboratory plasma (HEDLP) experiments, particle cancer therapy, etc (Roth *et al*., 2001; Roth *et al*., 2002; Roth *et al*., 2009; Patel *et al*., 2003; Bartal *et al*., 2011; Henestroza *et al*., 2011; Yang *et al*., 2010; Borgheshi *et al*., 2010; Romagani *et al*., 2008). Beam collimation, which is a

special case of focusing, is also needed for density radiography or injection into a transport lattice of a conventional accelerator.

Presently, the common technique to focus an ion beam is based on applications of externals magnetic or electric fields, generated by solenoids, quadrupoles, rf systems, plasma lenses, etc (Harres *et al*., 2010; Nishiuchi *et al*., 2010; Basko *et al*., 2008; Tauschwitz *et al*., 1995; Seidl *et al*., 2008; Ter-Avetisyan *et al*., 2008). In this paper we evaluate the technical feasibility of a novel passive focusing technique, which makes use of the beam's self-generated magnetic field. The physics prerequisite of the concept is straightforward: as a non-neutralized charged particle beam propagates in vacuum, it interacts with its self-generated fields: *defocusing* electric field, E, and *focusing* magnetic field, B (see Equation 1). In vacuum, the electric repulsing force is always stronger than the magnetic one. The excessive electrostatic force together with the emittance contribute to transverse expansion of the beam. If the electrical force is attenuated (or neutralized) then the beam is self-focused by the magnetic force.

$$F_E(r) = qE(r) = \frac{qI(r)}{2\pi v r},$$
$$F_B(r) = -qvB(r) = -\frac{q\mu_0 vI(r)}{2\pi r},$$
$$\left|\frac{F_B}{F_E}\right| = \frac{v^2}{c^2} = \beta^2.$$

Equation 1: Forces acting on a charged particle, *q* in a beam at a distance *r* from the axis. *I(r)* is axial current distribution, *v* is particle velocity.

Although the described principle seems straightforward, so far there is no convincing experimental confirmation of the phenomena with heavy ion beams. This phenomena is very well known in the beam physics of electrons: an electron beam, which usually has $v \approx c$, does not expand, due the favorable F_B/F_E relation the Equation 1. In addition, utilizing thin conducting surfaces to passively focus a particle beam has been analyzed and experimentally demonstrated for electrons (Fernsler *et al.,* 1990; Humphries *et al.,* 1989; Adler *et al.,* 1982). In this case, semi-transparent metal meshes are employed in place of foils. Numerous schemes to focus ion beams using fine conducting wires, meshes, and other structures to attenuate the defocusing self electric field, and/or utilizing plasma to produce neutralization, have been proposed in the community; many of these were associated with studies in collective ion acceleration (Olson *et al.,* 1979; Seidl *et al.,* 2008). In general, few documentation of these ideas is available and situation is even worse with finding the documented experimental outcomes. Recently, foil focusing for heavy ions and protons using the stack of a conductors has been proposed by B.G. Logan (Logan, 2010) to focus a heavy ion beam to a small spot, for the purpose of igniting the X-target (Henestroza *et al.,* 2011) in heavy-ion fusion and various fast ignition and warm dense matter applications. This paper has been triggered by the work of Henestroza *et al.,* 2011 and Logan, 2010 and its primary motivation is investigation of technical feasibility of experiments in which a clear experimental evidence of the self-focusing phenomena with heavy ion can be demonstrated.

The outline of this paper is as follows. First, physics of the concept is described; second, justification for the target-normal-sheath-acceleration (TNSA) protons (Snavely *et al.,* 2000; Hatchett *et al.,*2000; Borghesi *et al.,* 2004; Flippo et al., 2007, Brambrink et al., 2006) as the best candidate for the proof of principle experiments; third, technical feasibility study is presented, followed by a robust target design for the near term validation experiments.

2. Principle

The discussed approach to attenuate the electrical field is based on a well-known phenomenon: as a charged particle beam propagates between two closely spaced, conducting planes, separated by an insulator (later referred as a "gap"), the planes charge up with image charges of an opposite sign. The induced electric field from the image charges, E_{im} , is opposite to that of the beam, *E,* thus reduces the net field; meanwhile the magnetic self-field, *B,* of the beam remains unaffected by the conductors. The strength of this canceling E-field is determined by the distance between planes: a smaller distance results in a stronger field. The E-field attenuation produced by one pair of conductors is often not sufficient to produce a significant focusing (especially if the ions have an initial defocusing radial momentum) – the cancelation of the beam's self-electric field should be maintained for a distance long enough for the self-magnetic field to produce noticeable focusing. In practice, this can be implemented by placing (stacking) multiple conducting foils (later also referred as a lens) in the beam path with the distance between foils determining the effective focusing strength of such a lens.

Conductors are also essential to prevent ion beam current neutralization by the co-moving "knock-on" electrons produced during collisions of ions with a conductor. If not removed, the co-moving electrons neutralize the ion current thus weaken the magnetic field and the self-focusing. The absorbed electrons accumulate at the conducting plates and may disturb the charging induced by the beam. This excessive charge can be removed by grounding each conductor.

Precise analytical derivation of the electric field and the resulting beam envelope, in which the self-electric defocusing force is calculated for self-similarly evolving density profiles using Green's function, are extensively covered in an accompanying paper by Lund *et al.,* 2012. Strength of the net electrical field, a sum of the image charge field and self-field, is determined by the aspect ratio between transverse size of the beam and longitudinal distance between planes, *L* (from here on we assume a Gaussian transverse ion beam profile, with a beam radius equal to $2\sigma_r$; furthermore, σ_r/L is defined as the aspect ratio). In summary, the longitudinal electrical field has a bell shape distribution (Figure 2a); it is zero at the conductors and reaches maximum in the middle of the gap. Along the radial direction, the field increases with a distance and reaches a maximum at the edge of the beam (Figure 2b). Figure 3 shows attenuation of the E-field relative to the vacuum value – when no conductors are present – versus σ_r/L. The electrical field diminishes non-linearly with increasing ratio: the field is reduced to the quarter of its vacuum value when the distance between foils equals beam diameter and becomes negligible, less than a percent, when the distance is 1/8 of the beam radius. An important implication of Lund's calculations is that, since a typical radius of an ion beam ranges

from hundreds of micrometers to several millimeters, significant field attenuation can be achieved with macroscopic distances between foils.

3. Application to TNSA protons

Among various types of ion beams available for the validation of the described technique, TNSA proton beams are the most suitable candidates. First, the kilo-Ampere levels of electrical currents, typical for TNSA beams, are already sufficient to generate strong magnetic fields Lund *et al.,* 2012. Second, emittance of the TNSA beam ($\varepsilon \leq 0.1\pi$ mm mrad) is remarkably low for a typical high current ion beam. According to our literature survey, the "high" emittance of ion beams plausibly has been one of the major reasons preventing experimental demonstration of the concept with ion beams (Olson *et al.,* 1979). Third, high TNSA proton energies (1 MeV-50 MeV), lead to a more favorable magnetic-to-electric-force ratio, which scales as β^2 (Equation 1). In addition, MeV-energy protons can propagate with relatively low distortion through micrometer thick foils, making target manufacturing more simple and target handling easier. Lastly, since the number of knock-on electrons, generated during collisions of charged particles with a conductor scales as Z_{ion}^2, the unfavorable beam neutralization is least possible in experiments with protons (Hubbard *et al.,* 1979). Among major drawbacks of the TNSA beams that can prevent an observation of the phenomena are large energy spread (up to 100%), large beam divergence (10°-20° half angle) and beam distortion (energy loss and scattering).

A typical TNSA proton beam has ~5ps, FWHM pulse duration and an energy spectrum with a sharp exponential distribution (Figure 4) (Snavely *et al.,* 2000; Hatchett *et al.,* 2000; Borghesi *et al.,* 2004). Due to the broad energy range, protons of different energies arrive at the lens entrance at different times (see Figure 5). As the result, an instant electrical current in the lens depends on proton energy, leading to chromatic aberrations – protons of different energies are focused unequally and at different points. In the preliminary estimate, which assumes an initially collimated beam and 100% electric field neutralization, it was determined that, for example, a 25 MeV-energy protons (I~3A) from the high-energy part of the spectrum, can be focused in ~300 mm distance, while, less energetic but more intense, 1 MeV-energy protons (I~300 kA), can be focused in a ~30 mm distance. Such a large spread in the focal distances makes the design of an achromatic lens overly complex. For the initial proof-of-principle experiments it is preferred to design a simpler lens that is tuned for a narrow energy spectrum. Having analyzed various energies between 1 MeV and 20 MeV, the *10 MeV*-energy protons (I~400 A) are chosen as the base-line energy. These protons have sufficient current to pinch within a reasonable distance, require a technically feasible distance between conductors and number of conductors, and arrive at the lens before it gets destroyed be preceding protons (see more explanation below).

4. Proof-of-principle experiments

In a typical TNSA experiments, a proton beam is generated by illuminating a 5 μm -10 μm-thick, flat gold foil with an intense laser beam (100 fs - 500 fs pulse duraton, 10 J - 100 J energy per pulse, average laser power ~10^{18} W/cm^2) focused to >20 μm spot (Snavely *et al.,* 2000; Hatchett *et al.,*2000; Borghesi *et al.,* 2004). A typical divergence

of 10 MeV protons generated with a flat source foil is ~20° (half angel). As the TNSA proton beam propagates from a source foil, it is space-charge-neutralized by the electrons generated during the TNSA process and expands ballistically. Upon entering the lens, all the co-moving neutralizing electrons are stripped at the first foil and the proton beam becomes space-charge-dominated. At this stage the only force that can contain the beam is the self-magnetic force from the beam current. However, since the ions already possess a large transverse momentum (due to the large divergence), the magnetic force must first overcome the outward proton motion before it can start focusing the beam inward. The magnetic force is proportional to the current density, which is at its highest value when a lens is positioned to the source as close as possible. The closest distance that does not perturb the TNSA mechanism is ~0.5 mm, which for the 10 MeV protons corresponds to $2\sigma_r$ ~200 μm beam radius at the entrance of the lens. In this case, the ratio between electric and magnetic forces at the entrance of the lens is approximately 50:1. According to Figure 3, the 1:1 ratio, (a collimation case, when E-fled equals B-field) can be achieved when $2\sigma_r/L=2$, which corresponds to L~100 μm. Gap sizes less then this threshold value will result in the pronounced focusing.

The finite longitudinal extension of the proton bunch imposes limitation on the distance between conductors: for the optimal E-field neutralization, the beam must fill the entire space between conducting planes (Figure 1). A simple estimate shows that a 5 ps, 10 MeV beam has a ~400 μm length. The later number is thus a reliable estimation of the upper limit of distance between two neighbor conductors and does not interfere with the earlier 100 μm distance estimate necessary for the 1:1 ratio.

A careful analysis, presented in greater details in Lund *et al*., 2012, reveals a major issue that requires modifications of the TNSA flat-foil proton source. According to beam envelope calculations, beam divergence, as large as a fraction of a degree, results in a substantial increase in the focal length, even with complete E-field attenuation. The number of conductors, required to maintain the attenuation at these longer distances, exceeds the permissible number (estimated later). The 20° divergence of 10 MeV is far above the divergence threshold derived in Lund *et al*., 2012, making the observation of the pinch phenomena highly unlikely. At the same time, the same analysis shows that a slight inward focusing greatly aids the magnetic field, leading to a pronounced pinch at shorter distances.

One way to address the large divergence is to use a curved source foil (hemisphere shape), which is a well-known technique to focus a TNSA proton beam (Patel *et al*., 2003). A small focal spot (~ Ø20 μm) is desired in most applications, in which such a curved source foil is used. It is achieved with a hemisphere of a radius ranging from 100 μm to 160 μm. Meanwhile, in the "stack foil" setup, such a strong focusing is undesirable because it will lead to premature destruction of the lens. A proton source that will satisfy requirements of the proposed experiment must produce a collimated or slightly inward focused beam. Theoretically, such beams can be generated by hemispheres with R >160 μm. However, as the most of the experiments have been requiring strong focusing, there is no information available on the performance of hemisphere sources with R >200 μm. Up to date, the only available reference, is a PIC-code simulation (Bellei *et al*., 2012) that

demonstrates that a 10 μm thick, 300 μm radius hemisphere would produce a nearly collimated Ø75 μm diameter proton beam at ~400 μm distance from the source. Since there are no other references on the performance of a 300 μm radius source, results of this simulation are considered as the initial beam conditions at the entrance of the lens in the following lens design.

The beam envelopes for the three different constant spacing, 25 μm, 50 μm and 100 μm, are shown for a proton beam with the initial beam conditions from Bellei *et al*., 2012. While, in practice the gap size can have any value, these spacing are chosen to represent three typical cases. The 25 μm gap leads to a strong E-field attenuation (short focus) and indefinite beam confinement, which consists of periodic focusing and defocusing of the beam. The 50 μm spacing provides less attenuation, which results in a longer focal length, but still makes it possible to contain the beam. The 100 μm distance does not provide enough E-field cancelation to focus the beam and can only decelerate the space-charge driven expansion. For a reference, beam envelopes with a fully neutralized E-field and space charge dominated beam (i.e. no conductors) are also shown in the plots.

The beam envelopes estimates, shown in Figures 6 and 7, are idealized and do not consider scattering, full energy spectrum, finite length of the beam, etc; also the number of foils is unlimited. More precise beam envelope calculations and computer simulations that include some of these effects are partially covered in Lund's paper and match the data in Figures 6 and 7 within ~20%. This accuracy is sufficient for narrowing down design parameters for the initial experiments, in which any measurable spot-size-reduction is sufficient to prove the principle.

The E-field cancelation phenomena can be robustly observed by comparing radius in experiments with and without a lens (called a "reference" experiment) as it is schematically explained in Figure 8. For example, if a radio-chromic-film (RCF), a standard technique to measure beam profile in TNSA experiments, is placed 10 mm away from the source, diameter of the beam in the reference experiments is ~2 mm, while diameters in experiments with the various lenses are 120 μm, 200 μm and 400 μm (correspond to 25 μm, 50 μm and 100 μm spacing respectively) – a several folds difference that can be easily detected. Moreover, even the relative difference among experiments with various gap sizes, although less sensitive, is still large enough to be measured. The number of foils required for these initial proof of experiments, depending on the gap size, ranges from 100 to 400.

6. Considerations for the lens construction

In this section we discuss the hardware characteristics that can fulfill the physics requirement determined in the previous section.

In general, a “conducting plane” is a high conductivity and low inductance structure, such as a metal foil, metal mesh, carbon-fiber array, a slice of metal foam, etc. Aluminum is an obvious choice of the material, since it is easy to handle, it is a light-weight conductor and has the lowest energy loss and hence largest penetration range – long range is critical when a large number of conductors must be used. Aluminum is also a favorable material

from the radioactive activation safety point of view. Furthermore, since the number of knock-on electrons scales linearly with atomic number, Z_{foil}, aluminum, due its low Z_{foil}, will generate the least number of electrons (Hubbard *et al*., 1979), thus a lens made of aluminum will have less of the beam neutralization issue. The second best material option is carbon, which is mechanically more robust but has worse conductivity and higher energy loss.

Aluminum is also a suitable material for the lens fabrication using a chemical etching process, a possible procedure for thin foil production. The chemical etching process has been demonstrated recently at TU-Darmstadt (Schaumann, 2011) to fabricate stacks of ~1 μm thick Al foils separated by gaps with >20 μm between adjacent foils, and with a ~10 mm characteristic transverse extent. Another approach to fabricate a lens is to stack washers with Al-foils glued on each washer. The foils are pre-cut from a larger piece; thickness of a washer determines the gap size. Initial assembly tests by General Atomics indicate that construction of such a target is possible (Alexander, 2012). Because the main purpose of the foils is to attenuate the radial electric field, alignment tolerances (tilts, offsets, distortions) are not anticipated to be demanding so long as neighboring foils do not touch.

As discussed earlier, for the strongest image charge field, the size of a conductor must be much larger than the beam diameter. Considering the anticipated beam dimensions in Figure 7, foils larger than 5 mm will ensure that weakening effect of the fringe filed, occurring at the edges of a foil, is negligible. Thickness of the foil is a compromise: it must be sufficiently thin to minimize the beam distortion, such as scattering and energy loss, but at the same it must be sufficiently thick so that a foil is mechanically stable and can absorb all the co-moving electrons. The thinnest available freestanding metal foil is ~ 50 nm. Nevertheless, at least a 0.5 μm thick aluminum foil is necessary to stop 100 keV knock-on electrons (energy of knock-on electrons is not known; conservatively, if one assumes that a 10 MeV proton transfers a small fraction of its energy, then the energy of electrons should not exceed few hundreds of keV).

The maximum number of foils is limited by the distortion of the beam. The penetration range of a 10 MeV proton in solid aluminum is ~650 μm (SRIM, 2012): the deposition rate is low and quasi-constant (0.8 keV/ μm) for the first 500 μm of propagation, followed by an exponential increase, which peaks at 650 μm. For a reference, 1300 foils (0.5 μm-thick) will absorb the beam entirely, while1000 foils will absorb ~0.4 MeV (4%) – an insignificant beam distortion. Hence an upper limit of foil layers is between 1000 and 1500. For simplicity, in the future references 1000 foils can be used as a robust upper limit.

Lateral straggling, or scattering, is another effect that affects the proton beam and in addition to space-charge and emittance, it can be considered as an additional "force", contributing to the expansion of the proton bunch. According to TRIM, lateral straggling in a single, 0.5 μm thick, foil is ~5 nm, which corresponds to a ~0.1° divergence (SRIM, 2012). The net scattering of a proton beam in an Al plate, thickness of which is equivalent to 1000 foils stacked together, is ~40 μm, corresponding to ~4.5°. This

distortion would cause a noticeable broadening of an otherwise unperturbed beam and should be accounted in a lens design. Meanwhile, the effect of scatterings is less of an issue in the initial proof of principle experiments, as the expansion of the beam caused by straggling is still much smaller than the expansion of a beam in the reference experiment, in which no lens is present.

Preliminary estimates indicate, that total energy contained in a TNSA proton bunch (Figure 4) is sufficient to evaporate foil material along the path of the beam, making the lens a single-shot component. Due to the finite distance, between source and the lens and broad energy spread, different energies will arrive at different times (see Figure 3) thus allowing for a time window, during which the base-line, 10 MeV protons can propagate through an undamaged stack. Considering the known values of Al heat capacity, dE/dx and proton energy spectra in Figure 3, it is possible to estimate the temperature of foils at different moments of time. Summarized, all the protons between 10 MeV and 20 MeV contain energy sufficient to slightly pre-heat a foil to tens of degrees. For a reference, 10^{10}, base-line 10 MeV, protons deposit roughly 0.5 μJ in each foil, resulting in several degrees temperature increase. Arriving later, the low energy, high intensity protons ($N\sim10^{13}$) will heat up a foil to a plasma state, $T > 1$ eV. With the sound speed at a few km/sec, a hydro expansion time of a 0.5 μm thick foil is ~200 ps. For a comparison, it would take ~10 ns for the Al plasma to expand and fill in the smallest 25 μm design gap between conductors. At the same time, it takes ~300 ps for the entire proton bunch to propagate through a 10 mm long lens. Since the time-of-flight though the lens is close to the hydro-response time, the low energy protons will propagate through a hot plasma at a near solid state density in a warm-dense-matter (WDM) state. Conductivity of WDM is lower than that of cold matter, but it is much larger than that of an insulator. The exact WDM conductivity is not known, but plausibly it may be sufficient to generate image charge to focus the high intensity part that was not considered initially. Further investigations, based on WDM simulations, are needed, but in overall the initial estimates suggest that in the future due to the short-pulse nature of the processes, it might be possible to focus a broader energy spectrum of the TNSA proton beam – an achromatic proton lens.

Finally, an electrostatic case has been considered here, meaning that the image charge can form instantaneously. In reality, the time for a charge within a foil to respond to the external electrical field is finite, and if the pulse duration is much shorter than the response time, then the image charge will not accumulate in time, reducing the effectiveness of the E-field cancelation. The fastest response time of electrons in a typical conductor ($n_e=10^{21}$) is determined by the plasma frequency which is equal to $2\pi/\omega_p \sim 10^{-3}$ ps. This response time is noticeably less than the 5 ps bunch duration and thus justifies the electrostatic treatment.

7. Discussion

According to Lund *et al*., 2012 the theoretical limit of a focal spot size of a lens with constant pattern of foil spacing is ~50 μm. For a contrast, an estimate of emittance limited spot performed in Patel *et al*., 2003 is ~1 μm. The large discrepancy can be explained by the non-optimal, constant spacing pattern between conductors: as the beam

gets focused, aspect ratio changes unfavorably, resulting in less of E-field attenuation. Clearly, a progressively decreasing gap size is needed in order to keep the E-field attenuation (or aspect ratio) at the same constant level. Hence, in the future work, focal spots smaller than those quoted in Patel *et al*., 2003 can be plausibly achieved with an alternating, adaptive gap-size pattern, so that the attenuation of the electrical field (aspect ratio) is maintained at a constant rate.

A noticeable distortion of a beam in 0.5 μm Al foils is one of the key factors that determines a maximum number of foils. While, the degree of distortion is sufficient for the proof of principle-experiments, future lens optimizations will have to explore thinner conductor options, such as carbon fiber based foils, metal foams, etc. The thickness of Al can be further trimmed if the energy of knock-on electrons were known more accurately: the 100 keV is an overly conservative estimate. Hence, future experiments and simulations should concentrate on more precise estimates of the energy of the knock-on electrons. Further upgrades that can potentially improve performance of a lens include usage of ferromagnetic material and application of external magnetic fields (Lund *et al*., 2012).

An extensive 3D simulation, which includes full spectrum of the beam, ion scattering, electron neutralization, finite length of the beam, is needed for both the interpretation of near term experiments and a design of a lens tailored to a specific application. Additionally, a simulation that considers WDM aspect of foils, such as hydro-expansion and electrical conductivity, is necessary to develop an achromatic lens that can focus a broad spectrum of proton energies.

Finally, the described technique is not limited to only the TNSA protons. TNSA protons are a platform for demonstration of the principle, intended to stimulate application of the technique to other types of ion beams.

8. Summary

TNSA protons have been considered as a promising candidate to demonstrate the E-field cancelation phenomenon of an intense ion beam using a stack of conducting foils. A robust point design for the near term experiments consists of a few hundred, aluminum, 0.5 μm thick foils with gap sizes ranging from 25 μm to 100 μm. High divergence of TNSA beam requires, pre-collimation of the beam, which can be achieved with a curved source foil. A lens with these specifications as well as a curved source foil is within manufacturing capabilities of modern target fabrication labs. Experiments with the robust target design are the first step towards controlled focusing of ions with a stack of conductors.

Acknowledgments.

Author would like to thank Joe Kwan (LBNL), Christopher McGuffey (UCSD), Claudio Bellei (LLNL), Andy Faltens (LBNL) and Oliver Deppert (TU-Darmstadt) for the fruitful technical discussions. This research was performed under the auspices of the U.S. Department of Energy at the Lawrence Berkeley and Lawrence Livermore and National Laboratories under contract numbers DE-AC02-05CH11231 and DE-AC52-07NA27344.

Finally, the authors sadly note the untimely passing of our friend, colleague, and co-author Frank Bieniosek. His clarity of scientific vision, his energy and enthusiasm, his guidance, and his companionship are much missed.

References

M. Roth, A. Blazevic, M. Geissel, T. Schlegel, T. E. Cowan, M. Allen, J.-C. Gauthier, P. Audebert, J. Fuchs, J. M. ter Vehn, et al., *Phys. Rev. ST – Accel. Beams* **5**, 061301 (2002).

M. Roth, T. E. Cowan, M. H. Key, S. P. Hatchett, C. Brown, W. Fountain, J. Johnson, D. M. Pennington, R. A. Snavely, S. C. Wilks, *Phys. Rev. Lett*. **86**, 436 (2001).

M. Roth, I. Alber, V. Bagnoud, C. R. D. Brown, R. Clarke, H. Daido, J. Fernandez, K. Flippo, S. Gaillard, C. Gauthier, M. Geissel, S. Glenzer, G. Gregori, M. Günther, K. Harres, R. Heathcote, A. Kritcher, N. Kugland, S. LePape, B. Li, M. Makita, J. Mithen, C. Niemann, F. Nürnberg, D. Offermann, A. Otten, A. Pelka, D. Riley, G. Schaumann, M. Schollmeier, J. Schütrumpf, M. Tampo, A. Tauschwitz and An. Tauschwitz, *Plasma Phys. Control. Fusion* **51**, 124039 (2009).

P. K. Patel, A. J. Mackinnon, M. H. Key, T. E. Cowan, M. E. Foord, M. Allen, D. F. Price, H. Ruhl, P. T. Springer, and R. Stephens, *Phys. Rev. Lett*. **91**, 125004 (2003).

T. Bartal and et. al, *Nature p*. doi:10.1038/nphys2153 (2011).

X.H. Yang, Y.Y. Ma, F.Q. Shao, H. Xu, M.Y. Yu, Y.Q. Gu, T.P. Yu, Y. Yin, C.L. Tian and S. Kawata (2010). Collimated proton beam generation from ultraintense laser-irradiated hole target. Laser and Particle Beams, 28, pp 319-325 doi:10.1017/S0263034610000248

M. Borghesi, G. Sarri, C.A. Cecchetti, I. Kourakis, D. Hoarty, R.M. Stevenson, S. James, C.D. Brown, P. Hobbs, J. Lockyear, J. Morton, O. Willi, R. Jung and M. Dieckmann (2010). Progress in proton radiography for diagnosis of ICF-relevant plasmas. Laser and Particle Beams, 28, pp 277-284 doi:10.1017/S0263034610000170

L. Romagnani, M. Borghesi, C.A. Cecchetti, S. Kar, P. Antici, P. Audebert, S. Bandhoupadjay, F. Ceccherini, T. Cowan, J. Fuchs, M. Galimberti, L.A. Gizzi, T. Grismayer, R. Heathcote, R. Jung, T.V. Liseykina, A. Macchi, P. Mora, D. Neely, M. Notley, J. Osterholtz, C.A. Pipahl, G. Pretzler, A. Schiavi, G. Schurtz, T. Toncian, P.A. Wilson and O. Willi (2008). Proton probing measurement of electric and magnetic fields generated by ns and ps laser-matter interactions. Laser and Particle Beams, 26, pp 241-248 doi:10.1017/S0263034608000281

E. Henestroza, B. G. Logan, and L. J. Perkins, *Phys. Plasmas* **18**, 032702 (2011).

K. Harres, I. Alber, A. Tauschwitz, V. Bagnoud, H. Daido, M. Gunther, F. Nurnberg, A. Otten, M. Schollmeier, J. Schtrumpf, *Phys. Plasmas* **17**, 023107 (2010).

M. M. Basko, A. A. Drozdovskii, A.A. Golubev, K. L. Gubskii, D. D. Iosseliani, A. V. Kantsyrev, M. A. Karpov, A. P. Kuznetsov, Yu. B. Novozhilov, O. V. Pronin, S. M. Savin, P. V. Sasorov, D. A. Sobur, B. Yu. Sharkov, and V. V. Yanenko, *Physics of Particles and Nuclei Letters*, 2008, Vol. **5**, No. 7, pp. 582–585.

A. Tauschwitz, E. Boggasch, D.H.H. Hoffmann, J. Jacoby, U. Neuner, M. Stetter, S. Stöwe, R. Tkotz, M. De Magistris and W. Seelig (1995). Heavy-ion beam focusing with a wall-stabilized plasma lens. *Laser and Particle Beams*, **13**, pp 221-229 doi:10.1017/S0263034600009344

P. A. Seidl, A. Anders, F. M. Bieniosek, J. J. Barnard, J. Calanog, A. X. Chen, R. H. Cohen,J. E. Coleman, M. Dorf, E. P. Gilson, D. P. Grote, J. Y. Jung, M. Leitner, S. M. Lidia, B. G.Logan, P. Ni, P. K. Roy, K. Van den Bogert, A. B. Sefkow, W. L. Waldron, D. R. Welch,"Progress In Beam Focusing and Compression for Warm-Dense Matter Experiments", Heavy Ion Fusion Symposium 2008, Tokyo, Japan, August 2–9, 2008.

S. Ter-Avetisyan, M. Schnürer, R. Polster, P.V. Nickles and W. Sandner (2008). First demonstration of collimation and monochromatisation of a laser accelerated proton burst. *Laser and Particle Beams*, 26, pp 637-642 doi:10.1017/S0263034608000712

S.M. Lund, R.H. Cohen, P.A. Ni, "Envelope model for passive magnetic focusing of an intense proton or ion beam propagating through thin foils", submitted to *Physical Review Special Topics*: *Accelerators and Beams* (2012)

M. Nishiuchi and et. al, *Phys. Rev. ST – Accel. Beams* **13**, 071304 (2010).

R. F. Fernsler, R. F. Hubbard, and S. P. Slinker, *J. Appl. Phys*. **68**, 5985 (1990).

S. Humphries, C. Ekdahl, and D. M. Woodall, *Appl. Phys. Lett*. **54**, 2195 (1989).

R. J. Adler, *Part. Accel*. **12**, 39 (1982).

C. L. Olson and U. Schumacher, Collective Ion Acceleration (Springer-Verlag, Heidelberg, 1979), springer tracts in modern physics vol. **84** ed.

B. G. Logan, October 26, 2010, Lawrence Berkeley Laboratory seminar (unpublished).

R. A. Snavely and et. al, *Phys. Rev. Lett*. **85**, 2945 (2000).

S. Hatchett, C. Brown, T. E. Cowan, E. A. Henry, J. Johnson, M. H. Key, J. A. Koch, A. B. Langdon, B. F. Lasinsky,R. W. Lee, et al., *Phys. Plasmas* **7**, 2076 (2000).

M. Borghesi and et. al, *Phys. Rev. Lett*. **92**, 055003 (2004).

K. FLIPPO, B.M. HEGELICH, B.J. ALBRIGHT, L. YIN, D.C. GAUTIER, S. LETZRING, M. SCHOLLMEIER, J. SCHREIBER, R. SCHULZE AND J.C. FERNÁNDEZ (2007). Laser-driven ion accelerators: Spectral control, monoenergetic ions and new acceleration mechanisms. *Laser and Particle Beams*, **25**, pp 3-8 doi:10.1017/S0263034607070012

ERIK BRAMBRINK, MARKUS ROTH, ABEL BLAZEVIC and THEODOR SCHLEGEL (2006). Modeling of the electrostatic sheath shape on the rear target surface in short-pulse laser-driven proton acceleration. *Laser and Particle Beams*, **24**, pp 163-168 doi:10.1017/S026303460606023X

C. Bellei, M. E. Foord, T. Bartal,1 M. H. Key, H. S. McLean, P. K. Patel, R. B. Stephens, and F. N. Beg,1 *PHYSICS OF PLASMAS* **19**, 033109 (2012).

R. F. Hubbard, S. A. Goldstein, and D. A. Tidman, ”KNOCK-ON ELECTRONS IN THE TARGET CHAMBER,”Proceedings of the Heavy Ion Fusion Workshop held at the Claremont Hotel, Berkeley, CA, October 29 – November9, 1979, pg 488; obtainable by Lawrence Berkeley Laboratory publication LBL-10301 and Stanford Linear Accelerator Laboratory publication SLAC-R-542.

G. Schaumann, private communication, 2011

A. Neil, private communication, 2012

SRIM - The Stopping and Range of Ions in Matter, 2012, www.srim.org

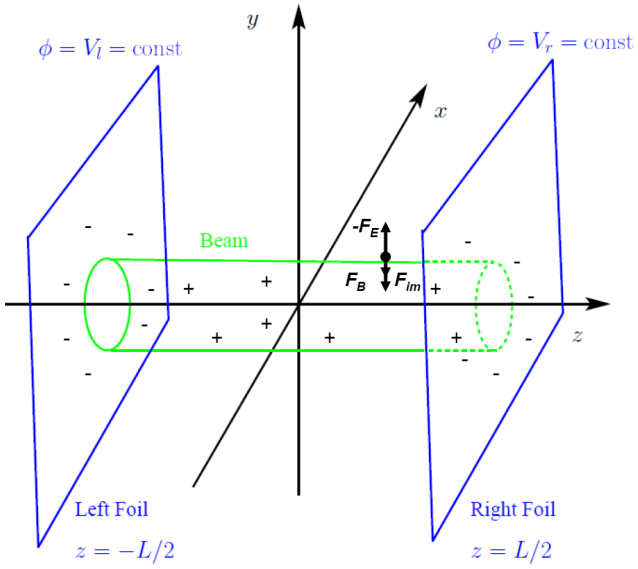

Figure 1:Axisymmetric beam between two, thin conducting foils located at z = ±L/2. The foils are grounded. As a beam propagates between two closely spaced, conducting planes, separated by an insulator (vacuum), the planes charge up with image charges. An electric field, E_{im} induced by this charge, is opposite to that of the beam, E and cancels it out; the magnetic self-field, B of the beam remains unaffected by the conductors, thus allowing for a pinch.

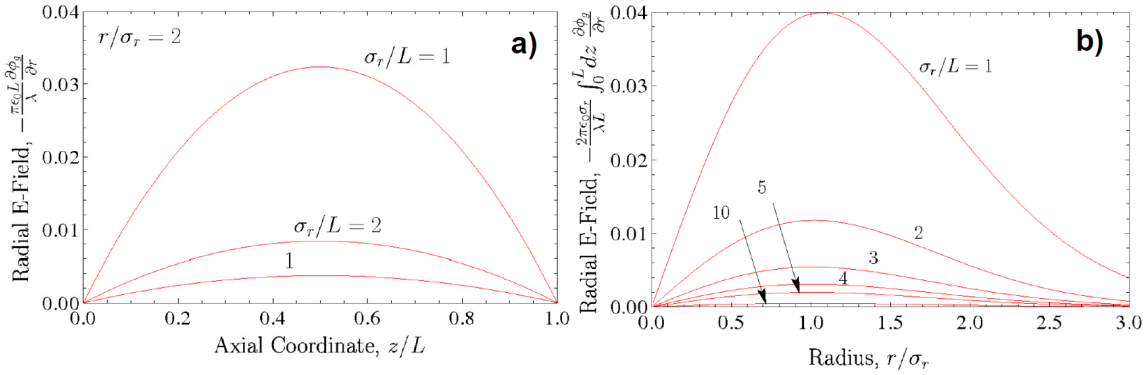

Figure 2: Longitudinal (a) and transverse (b) net E-field distribution between conducting planes shown for various beam-to-foils space aspect ratios (Lund *et al*., 2012). The transverse profile is shown for the middle point between conductors, z=0. For a reference, electrical field strength without conductors (σ_r/L=0) is 0.4.

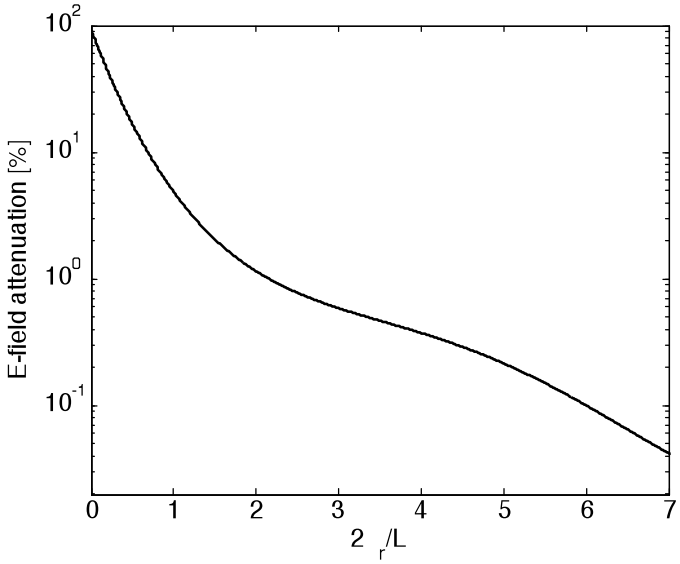

Figure 3: Relative strength of the net electric field between conductors versus aspect ratio. 100% corresponds to un-attenuated electrical field when no conductors are present ($\sigma_r/L = 0$). The attenuation curve is shown for ions in the mid point of the gap, x=0, at a 2σ distance from beam axis.

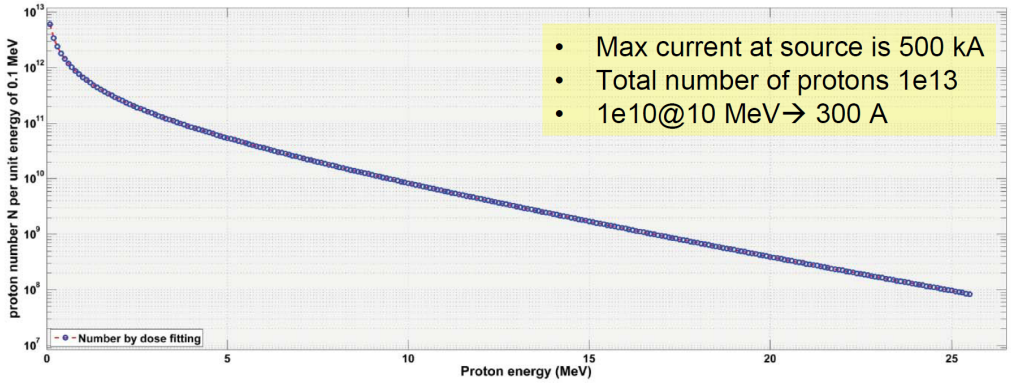

Figure 4: : Typical proton spectrum generated by PHELIX-GSI laser via TNSA mechanism.

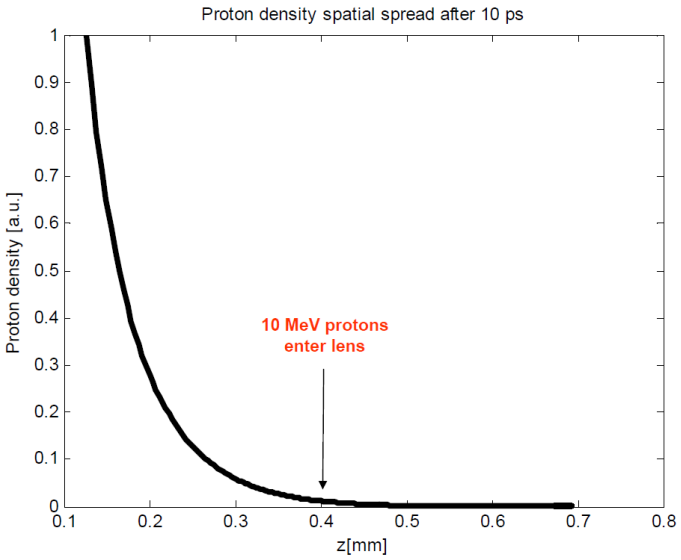

Figure 5: A spatial spread of 5 ps proton bunch at the moment, when the base-line, 10 MeV, protons enter the lens (positioned 0.4 mm away from the source). High-energy proton, arriving earlier, slightly pre-heat Al foils; low energy protons have sufficient energy to evaporate foils.

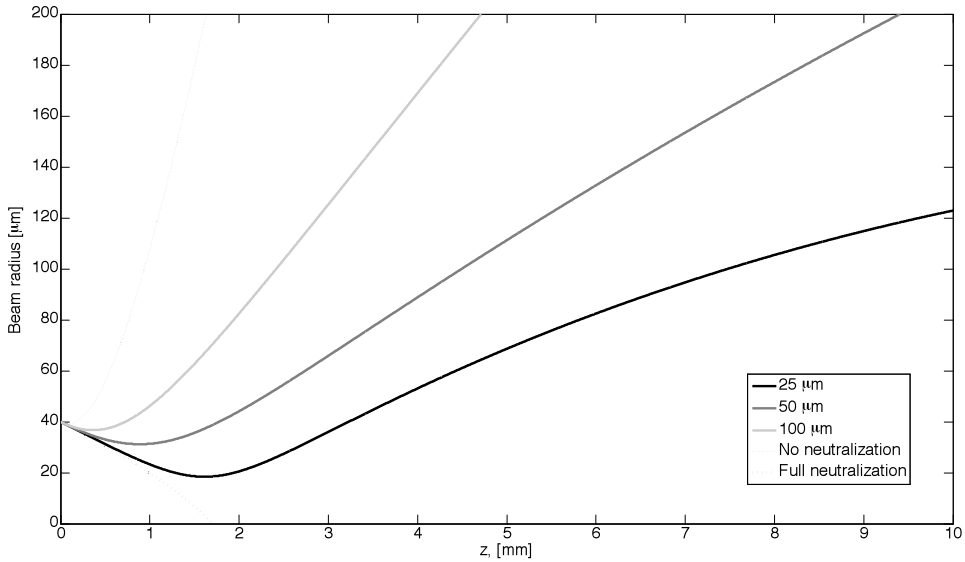

Figure 6: Estimates of beam envelope inside a lens with different distances between conductors. For a reference, beam envelopes with a fully neutralized E-field and space charge dominated beam (no conductors) are shown.

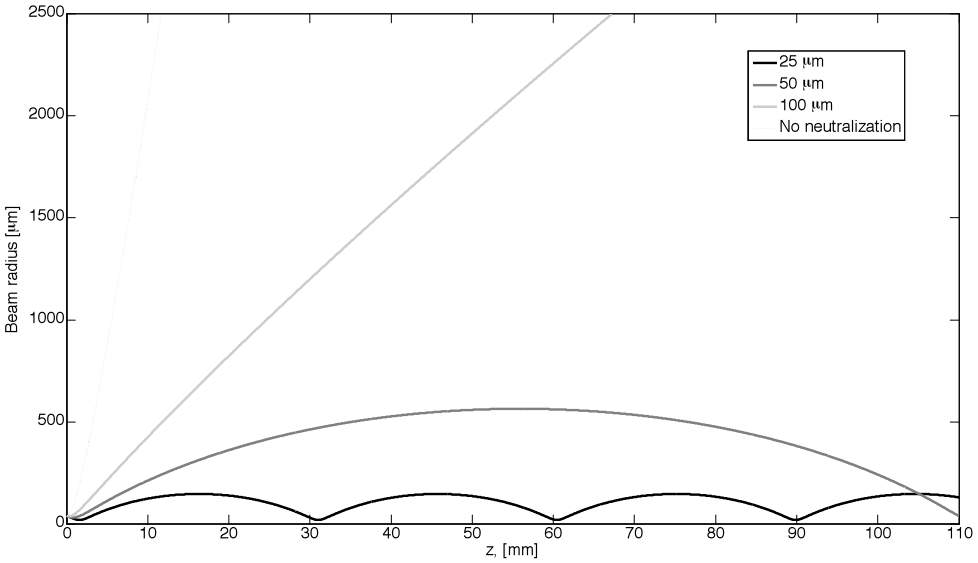

Figure 7: Estimates of beam envelope inside a lens with different distances between conductors (zoomed out).

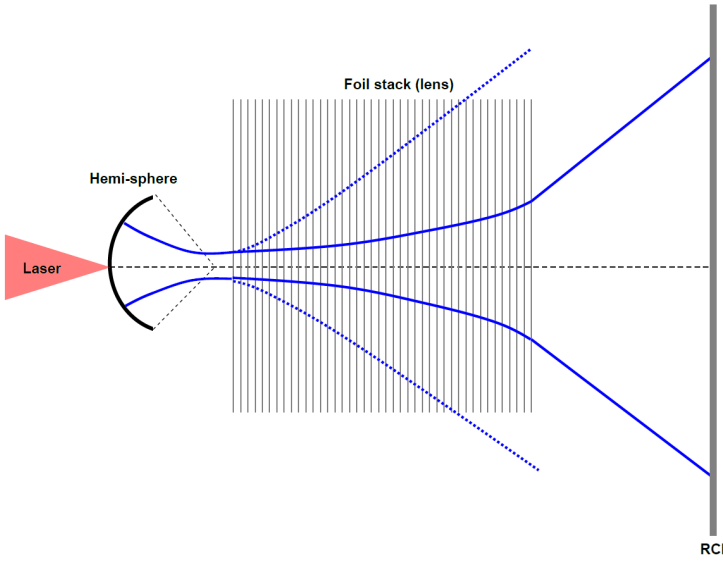

Figure 8: Scheme of a proof-of-principle experiments (not to scale). Dashed beam envelope represents the reference experiment, in which no lens is used and the beam expands ballistically.